

ORIGINAL ARTICLE

Repair of Avascular Meniscus Tears with Electrospun Collagen Scaffolds Seeded with Human Cells

Jihye Baek, PhD,^{1,2} Sujata Sovani, MS,¹ Nicholas E. Glembofski, BS,¹ Jiang Du, PhD,³ Sungho Jin, PhD,² Shawn P. Grogan, PhD,¹ and Darryl D. D'Lima, MD, PhD¹

The self-healing capacity of an injured meniscus is limited to the vascularized regions and is especially challenging in the inner avascular regions. As such, we investigated the use of human meniscus cell-seeded electrospun (ES) collagen type I scaffolds to produce meniscal tissue and explored whether these cell-seeded scaffolds can be implanted to repair defects created in meniscal avascular tissue explants. Human meniscal cells (derived from vascular and avascular meniscal tissue) were seeded on ES scaffolds and cultured. Constructs were evaluated for cell viability, gene expression, and mechanical properties. To determine potential for repair of meniscal defects, human meniscus avascular cells were seeded and cultured on aligned ES collagen scaffolds for 4 weeks before implantation. Surgical defects resembling “longitudinal tears” were created in the avascular zone of bovine meniscus and implanted with cell-seeded collagen scaffolds and cultured for 3 weeks. Tissue regeneration and integration were evaluated by histology, immunohistochemistry, mechanical testing, and magnetic resonance imaging. *Ex vivo* implantation with cell-seeded collagen scaffolds resulted in neotissue that was significantly better integrated with the native tissue than acellular collagen scaffolds or untreated defects. Human meniscal cell-seeded ES collagen scaffolds may therefore be useful in facilitating meniscal repair of avascular meniscus tears.

Introduction

AMONG KNEE INJURIES, meniscal tears are the most frequent type of injury and are an important factor of knee disability,^{1–3} accounting for up to 15% of all knee injuries in younger active individuals.⁴ Partial or total meniscectomy is currently the most commonly recommended treatment approach for meniscal tears.⁵ A number of techniques have been developed to repair meniscal tears: involving sutures, screws, arrows, and darts.⁶ These repair procedures can relieve pain, locking, and instability in the short term. However, in the long term, no significant benefit has been documented with respect to preventing degenerative joint changes and accelerated osteoarthritis due to deficient meniscal function.^{7,8}

The predominant issue with meniscal tears is the absence of self-healing capacity of the meniscus due to lack of vasculature.^{1,9} While fully vascularized at birth, adult menisci are only vascularized in the outer one-third to two-thirds.¹ The vascularized periphery of the meniscus possesses some

self-healing capacity and minor or simple tears can be repaired.¹⁰ However, large or complex tears, especially those within the avascular region, are extremely difficult to repair.

Numerous approaches have been attempted to enhance repair or replace injured meniscal tissue. Transplantation of meniscal allografts can relieve pain and enhance function in the short term.^{11–13} Others have explored replacing meniscal tissue using natural biomaterials, including periosteal tissue,¹⁴ small intestine submucosa,¹⁵ acellular porcine meniscal tissue,¹⁶ perichondrial tissue,¹⁷ and bacterial cellulose.¹⁸ However, these approaches have yet to be translated to clinical application largely because of the lack of replication of the organization, structure, and biological and mechanical properties of meniscal tissue.

Electrospinning makes it feasible to fabricate nanoscale fibers composed of synthetic materials such as polylactic acid (PLA) and polycaprolactone (PCL)^{19–21} and of natural materials such as collagen, gelatin, and chitosan.^{22–24} Electrospun (ES) fiber matrices have been used successfully

¹Shiley Center for Orthopaedic Research and Education at Scripps Clinic, La Jolla, California.

²Department of Material Science and Engineering, University of California, La Jolla, California.

³Department of Radiology, School of Medicine, University of California, San Diego, San Diego, California.

in drug delivery and wound healing, as well as other biomedical applications.²⁵ These nanofibrous scaffolds possess the advantage of tunable mechanical strength with a large biomimetic surface area. Cell attachment, cell proliferation, and transport of nutrients through the scaffold can be accelerated by the high surface-to-volume ratio and by the porous structure of the scaffold.^{26,27} We previously demonstrated that ES PLA scaffolds can replicate meniscus nanostructural and microstructural organization with appropriate mechanical properties and high cell compatibility.²⁸

Although synthetic polymers are biocompatible, they are known to cause significant inflammation and foreign body reaction when implanted *in vivo*.²⁹ For example, biodegradation products (lactic acid) released from PLA reduce pH within the knee joint.³⁰ Natural polymers may circumvent these complications and a scaffold composed of collagen may be optimal since it is the main fibrillar component of the meniscus, is biocompatible, and has been used in clinically approved/cleared devices.^{31,32}

The objective of this study was to develop biomimetic scaffolds, which replicate the collagen fibrils of native menisci, seeded with human meniscogenic cells, and with biomechanical properties approaching that of native meniscal tissue. Toward this objective, we used ES scaffolds composed of collagen type I with different fiber arrangements (random and aligned) to emulate the regional distribution of meniscal fibers. These ES scaffolds were then crosslinked to enhance mechanical properties and seeded with human meniscal fibrochondrocytes. The scaffolds were characterized by fiber morphology and biomechanical properties. The meniscogenic potential was assessed by cell viability, proliferation, gene expression, and matrix synthesis. To determine the potential for clinical translation, we also evaluated *ex vivo* repair by implanting cell-seeded ES scaffolds in tears created in the avascular region of live meniscal bovine explants.

Materials and Methods

Fabrication of ES collagen type I scaffold

Sixteen percent w/v Bovine Collagen type I (Semed S, acid-soluble, DSM, NL) was dissolved in 20× phosphate-buffered saline (PBS) and ethanol at a ratio of 1:1 w/w as previously described.³³ ES scaffolds were created in a similar way as previously described for ES PLA scaffolds.²⁸ The collagen solution was placed in a syringe, which was actuated by a syringe pump (KDS200; KD Scientific, Inc.) at a feeding rate of 0.1–0.2 mL/h into a Teflon tube that was connected to a 21-G needle with an inner diameter of 0.5 mm. Collagen fibers were ES on collectors covered by aluminum foil. For fabricating random fibers, a flat plate was used as a collector with a tip-to-collector distance of 16 cm. For fabricating aligned fibers, a drum, rotating nominally at 2400 rpm was placed at 12 cm from the needle tip (to the tangent surface of the drum). The applied voltage was varied from 15 to 20 kV by a voltage-regulated DC power supply (NNC-30 kV-2 mA portable type; NanoNC) to generate the polymer jet. ES collagen scaffolds were crosslinked by submerging in 0.25% glutaraldehyde (GA; Sigma-Aldrich) in 1× PBS for 1 h. After fixation, scaffolds were washed thrice for 10 min each with absolute ethanol and stored at 4°C.

Structural morphology of collagen type I scaffold

To examine the ultrastructural morphology of ES collagen type I scaffolds, scanning electron microscopy (SEM) was performed. The ES collagen scaffolds were coated with iridium using a sputter coater (Emitech K575X; EM Technologies Ltd.). The prepared scaffolds were examined under SEM (Philips XL30; FEI Co.) with an accelerating voltage of 10 kV. The diameter of the ES fibers for each scaffold was calculated from the SEM images by an image processing software (Image J; National Institutes of Health).

Tissue harvesting and cell isolation

Normal human menisci (medial and lateral) were obtained from tissue banks (approved by Scripps Institutional Review Board), from six donors (mean age, 29.8 ± 4.7; age range, 23–35 years; two females and four males). To grade and select the menisci, a macroscopic and histologic grading system was used.³⁴ The avascular region was defined as the one-third outer portion and the remaining two-third was considered the vascular region. These regions were separated by a scalpel and enzymatically digested using collagenase (2 mg/mL; C5138; Sigma-Aldrich) in Dulbecco's Modified Eagle Medium (DMEM) (Mediatech, Inc.) and 1% Penicillin/Streptomycin/Fungizone (Life Technologies) for 5–6 h. Digested tissues were filtered through 100-µm cell strainers (BD Biosciences) and seeded in monolayer culture in DMEM (Mediatech) supplemented with 10% calf serum (Omega Scientific, Inc.) and 1% Penicillin/Streptomycin/Gentamicin (Life Technologies). The isolated meniscal cells were cultured for one passage before seeding on ES scaffolds.

Cell seeding in ES collagen type I scaffold

Isolated human meniscus cells (passage 1) derived from the vascular and avascular regions were seeded on 2 cm × 1 cm rectangular random and were aligned on collagen scaffolds at a cell density of 0.5×10^6 per scaffold. Cell-seeded scaffolds were cultured in six-well plates and maintained in 2 mL of monolayer culture medium for 3 days to permit initial cell attachment and scaffold colonization. The medium was then changed to the serum-free ITS+ medium (Sigma) supplemented with 10 ng/mL transforming growth factor $\beta 1$ (TGF $\beta 1$; PeproTech). The serum-free ITS+ medium used for ES scaffolds culture consisted of DMEM (Mediatech), 1 × ITS+ medium (Sigma-Aldrich) (i.e., 10 mg/mL insulin, 5.5 mg/mL transferrin, 5 ng/mL selenium, 0.5 mg/mL bovine serum albumin, and 4.7 mg/mL linoleic acid), 1.25 mg/ml human serum albumin (Bayer), 100 nM dexamethasone (Sigma-Aldrich), 0.1 mM ascorbic acid 2-phosphate (Sigma-Aldrich), and penicillin/streptomycin/gentamicin (Gibco).³⁵ The scaffolds and cells were cultured for 2 weeks in the ITS+ medium with medium changes every 3–4 days. At 2 weeks, scaffolds were assessed for cell viability and cell distribution and morphology by histology and SEM.

Mechanical properties of collagen type I scaffold

The ES collagen scaffold mechanical properties were quantified by tensile testing ($n=8$ per group) as described previously.²⁸ The scaffolds were tested under three different conditions: (i) random and aligned ES dry scaffolds, (ii) aligned scaffolds seeded with avascular human meniscus

cells and cultured for 1 and 3 weeks, and (iii) aligned scaffolds without cells and cultured for 1 and 3 weeks. Scaffolds were cut into dog-bone-shaped specimens with a gauge length of 8 mm and gauge width of 2 mm using a custom-made aluminum template. The thickness of each scaffold was measured using a digital caliper. For mechanical testing of cultured cell-seeded scaffolds, human avascular cells (0.5×10^6 cells/sample) were seeded on the dog-bone-shaped aligned collagen scaffold. Scaffolds were cultured as described in the previous section.

The specimens were mounted in the grips of a uniaxial testing machine (Instron® Universal Testing Machine, 3342 Single Column Model) with a 500 N load cell and tested to failure at a displacement rate of 1 mm/s. Samples that failed outside the gauge length were discarded and then mechanical properties of the ES collagen scaffolds were quantified by tensile testing ($n=6$ per group). Young's modulus was calculated as the slope of the linear segment of the stress-strain curve. The maximum load before failure was recorded as the ultimate tensile strength (UTS).

Cell viability assessments

The viability of cells cultured on aligned collagen scaffolds was observed using Calcein-AM and Ethidium Homodimer-1 (Live/Dead kit; Life Technologies) and a laser confocal microscope (LSM-510; Zeiss) as previously described.²⁸

Cellular morphology of meniscus cells on collagen type I scaffold by SEM

SEM was employed to observe high-resolution features of cells grown on the ES collagen scaffolds. After 2 weeks in culture, cell-seeded scaffolds were washed with $1 \times$ PBS and fixed with 2.5% w/v GA (Sigma-Aldrich) in $1 \times$ PBS for 1 h. After fixation, specimens were washed thrice with PBS for 10 min each wash. Then, the specimens were dehydrated in a graded series of ethanol (50%, 70%, and 90%) for 30 min each and left in 100% ethanol for 24 h at temperatures below zero. Next, the specimens were kept in 100% ethanol until they were completely dried in a critical point dryer (Autosamdri-815, Series A; Tousimis, Inc.). The surface of dried samples was then metalized by sputter coating with iridium. The morphology of the scaffolds as well as that of the adherent cells was observed by SEM (Philips XL30).

Measurement of newly deposited collagen type I

Human meniscal avascular cells were cultured on discs of aligned collagen scaffolds (6 mm in diameter, 0.125×10^6 cells per disc) in the serum-free ITS+ medium (Sigma-Aldrich) supplemented with 10 ng/mL TGF β 1 (PeproTech) for 3 weeks with medium changes every 3–4 days. The scaffold and cells were solubilized with pepsin under acidic conditions and digested with pancreatic elastase at neutral pH to convert polymeric collagen to monomeric collagen at 2°C–8°C. To evaluate newly deposited collagen, an enzyme-linked immunosorbent assay (ELISA) was performed (Human collagen type I ELISA; MD Bioproducts). The plate was read on a SpectraMax 384 Plate Reader (Molecular Devices) at 450 nm (650 nm reference). Nonspecific ELISA readings were controlled by using noncell-seeded scaffolds cultured under the same conditions and times.

RNA isolation and RT-polymerase chain reaction

Total RNA was isolated using the RNeasy mini kit (Qiagen) and first-strand cDNA was made as reported by the manufacturer's protocol (Applied Biosystems). Quantitative RT-polymerase chain reaction was performed using TaqMan® gene expression reagents. *COL1A1*, *SOX9*, *COMP*, *CHAD*, *aggrecan (AGG)*, and *GAPDH* were detected using Assays-on-Demand™ primer/probe sets (Applied Biosystems). Expression levels were normalized to *GAPDH* using the recommended Δ Ct method, and fold change was calculated using the $2^{-\Delta\Delta Ct}$ formula.³⁶

Ex vivo meniscal repair

Avascular bovine meniscal tissue explants were harvested from fresh adult bovine knees and cultured in the medium for 5 days in six-well plates with DMEM supplemented with 10% calf serum and 1% Penicillin, Streptomycin, and Gentamicin. To simulate a longitudinal meniscal tear, a scalpel was used to cut the explant parallel to the circumferential direction of the collagen bundles. Aligned collagen scaffolds seeded with avascular meniscal cells were first cultured for 2 weeks and then inserted in the meniscal tear with the scaffold fibers aligned parallel to the circumferential collagen fibers of the host meniscal tissue. The repaired meniscal explants were maintained in the serum-free ITS+ medium (Sigma-Aldrich) supplemented with 10 ng/mL TGF β 1 (PeproTech) (8 mL/well) for an additional 3 weeks (with medium changes every 4–5 days) and processed for histology and magnetic resonance imaging (MRI) to assess filling of meniscal tear with neotissue and scaffold/host integration.

Histology, immunohistochemistry, and histomorphometry

Ex vivo meniscal explants with meniscal tears repaired with cell-seeded or acellular ES collagen scaffolds were fixed in Z-Fix (ANATECH) for 9 days and embedded in paraffin. Sections (5–7 μ m thick) were stained with hematoxylin and eosin for the study of morphological details, while Safranin O-fast green staining was used to assess glycosaminoglycan distribution. For detection of collagen type I by immunohistochemistry (IHC), cut sections were treated with hyaluronidase for 2 h³³ and incubated overnight at 4°C with a primary antibody against collagen type I (clone: I-8H5; MP Biomedicals) at 10 μ g/mL. Secondary antibody staining and detection procedures were followed as previously described.^{28,37} An isotype control was used to monitor nonspecific staining. To detect cells, sections were stained with the Vectashield mounting medium containing 4',6-diamidino-2-phenylindole (Vector Laboratories).

Microphotographs of all histological sections were captured using a microscope (Olympus BX60; Shinjuku) mounted with a calibrated charge-coupled device camera (Macrofire Optronics). Histomorphometric analysis was performed using the image processing software (Image J; National Institutes of Health). The total length of the interface between the meniscal tissue and scaffold was measured and classified as integration, disintegration, and apposition as described by Pabbruwe *et al.*^{38,39} Briefly, the presence of a gap between the scaffold and adjacent host tissue was classified as “disintegration.” Apposition of scaffold to adjacent

host tissue with clear demarcation of the interface was classified as “apposition.” Finally, a continuous interface with the absence of a clear boundary between scaffold and adjacent host tissue and the presence of cell migration and matrix remodeling was classified as “integration.” Each type of interface was expressed as a percentage of the total interface.

Magnetic resonance imaging

Bovine meniscus explants with surgically created tears were implanted with collagen scaffolds and cultured for 3 weeks as described above. Explants were divided into three groups: (i) untreated tears, (ii) tears repaired with acellular scaffolds, and (iii) tears repaired with cell-seeded scaffolds. An 11.7T system, Bruker BioSpec with 750 mT/m gradients was used. 2D multislice/multiecho pulse sequences (repetition time [TR]=30,000 ms, echo time [TE]=8.16 ms) of voxel size 50–70×50–70×500 μm were employed together with 3D multigradient echo sequences (TR=80 ms, TE=2–18 ms, fractional anisotropy [FA]=14°).

Mechanical testing of repair in ex vivo model

Bovine meniscus explants with untreated tears or tears repaired with cell-seeded or acellular scaffolds ($n=7$ per group) were tested for tensile mechanical properties. Human meniscus avascular cells were seeded on aligned collagen scaffolds and cultured for 2 weeks. Bovine menisci were cut into rectangular shapes (width: 12.24 ± 0.37 mm, length: 16.88 ± 1.85 mm, and thickness: 2.27 ± 0.26 mm). The average dimensions for each group are presented in Table 1. Surgical tears (nominally 10 mm in length) were made horizontally in the center of rectangular-shaped meniscus specimens and acellular or cell-seeded collagen scaffolds were inserted into the surgical defect. After 2 weeks in culture, the specimens were moved into 50-mL conical tubes and washed with 1×PBS. Each end of the specimen (with the longitudinal tear in the center) was mounted in the clamps of an Instron mechanical testing frame (Instron® Universal Testing Machine, 3342 Single Column Model). Tensile force was monitored using a 500 N load cell as samples were tested to failure in tension at a constant displacement rate of 1 mm/s. Young’s modulus was calculated from the slope of the linear segment of the stress–strain curve. The UTS was calculated at the maximum load before failure.

Statistical analysis

Analysis of variance, *post hoc* student’s *t*-tests, and Kruskal–Wallis and Mann–Whitney analysis were used to detect sta-

tistically significant differences in fiber diameter, mechanical properties, and gene expression levels. *p* values <0.05 were considered significant.

Results

Controlled production of ES collagen fibrous scaffolds

The morphological structure of aligned and random ES collagen fibers is shown in Figure 1A and B. The rotating drum speed (~2400 rpm) and delivery parameters used produced scaffold structures with a high degree of alignment.

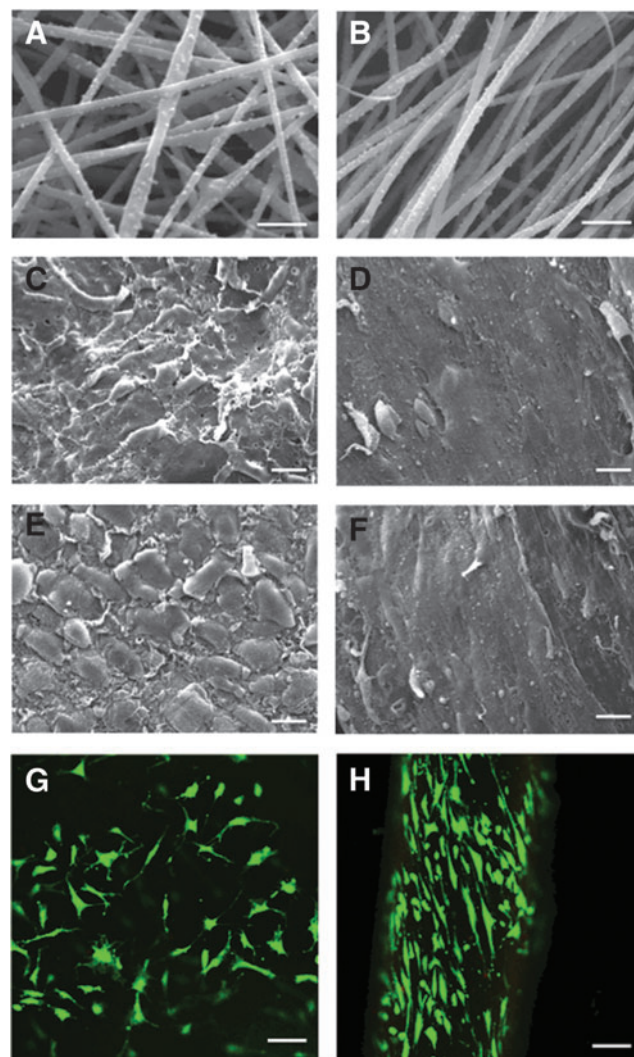


FIG. 1. Scanning electron micrographs (SEM) of electrospun (ES) collagen scaffolds and cellular response. (A) SEM of random and (B) aligned ES collagen fibers (Mag. 10,000×; scale bar: 2 mm). (C) SEM of vascular human meniscus cells cultivated on random and (D) aligned electrospun collagen fibers (Mag. 625×; scale bar: 20 mm). (E) Avascular human meniscus cells seeded on random and (F) aligned electrospun collagen fibers (Mag. 625×; scale bar: 20 mm). (G) Vascular human meniscus cells cultivated on random scaffolds and (H) avascular human meniscus cells on aligned scaffolds demonstrating viability (live/dead) and aligned cells cultivated on collagen scaffolds (Mag. 10×; scale bar: 200 mm in confocal images). Color images available online at www.liebertpub.com/tea

TABLE 1. DIMENSIONS OF EXPLANT MECHANICAL TESTING SPECIMENS FOR EACH CONDITION

	Only defect	Only collagen	Cell-laden collagen
Defect size	10.00	10.00	10.00
Width	12.23 ± 0.45	12.29 ± 0.35	12.21 ± 0.36
Length	16.30 ± 1.74	16.32 ± 1.55	16.34 ± 1.89
Thickness	2.22 ± 0.21	2.27 ± 0.18	2.48 ± 0.14

Defect size, width, length, and thickness for each condition expressed as mean ± standard deviation (mm, $n=7$).

The average diameter of aligned fibers was 496 ± 97 nm (range, 340–860 nm) and that for random collagen fibers was 467 ± 76 nm (range, 250–720 nm). The thickness of GA crosslinked random scaffolds was 0.25 ± 0.04 mm, while crosslinked aligned scaffolds were 0.25 ± 0.03 mm.

Scaffold organization influences cell response, while maintaining high cell viability

Meniscal avascular and vascular cells seeded upon randomly oriented ES collagen scaffolds were flattened and

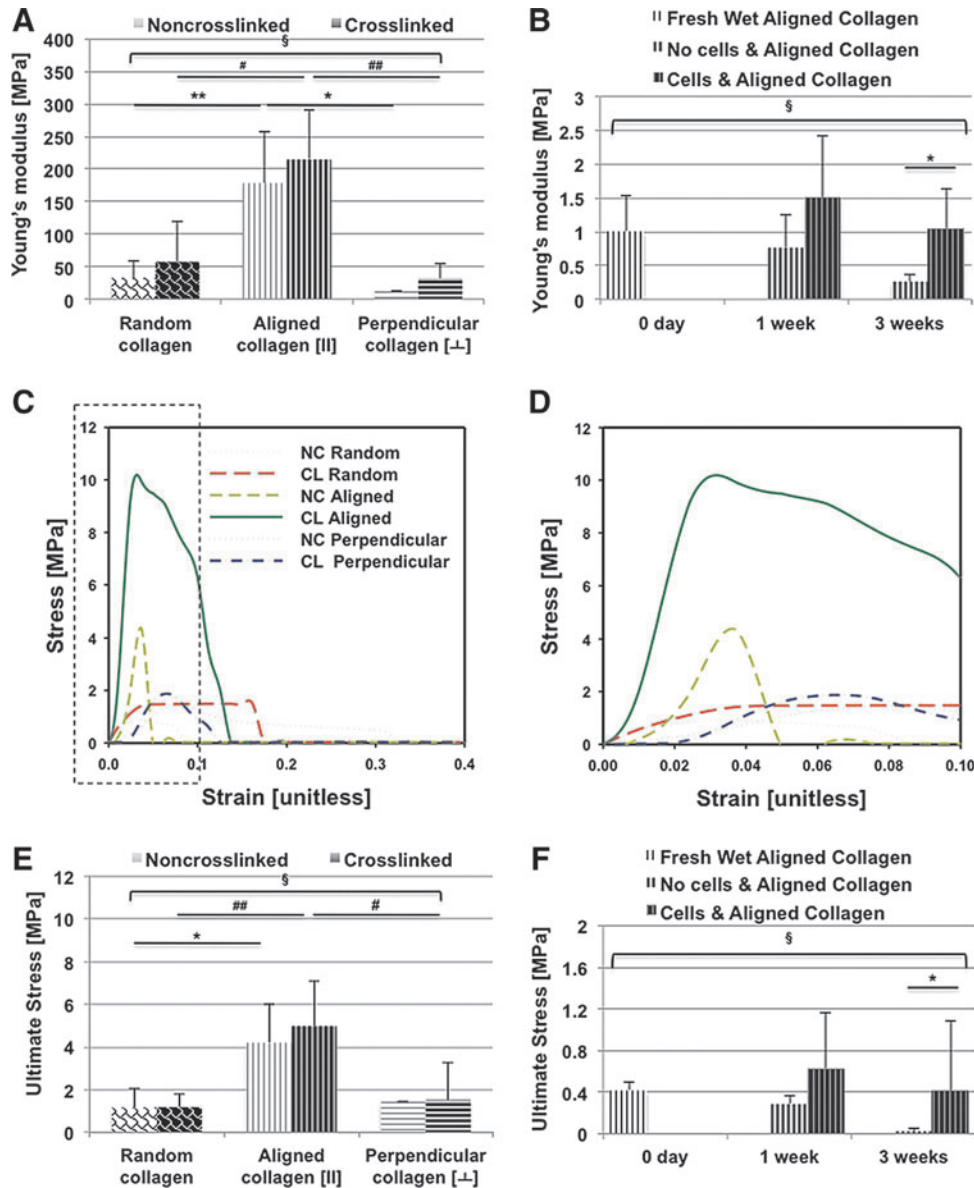


FIG. 2. Mechanical testing of random and aligned ES collagen scaffolds. **(A)** Young's modulus (MPa) for random, aligned (along fiber orientation), and perpendicular to fiber orientation with and without crosslinking ($n=8$). (** $p=0.0010$ noncrosslinked aligned vs. random collagen scaffolds, * $p=0.03$ noncrosslinked aligned vs. perpendicular oriented collagen scaffolds, # $p=0.005$ crosslinked aligned vs. random collagen scaffolds, ## $p=0.002$ crosslinked aligned vs. perpendicular oriented collagen scaffolds, Mann-Whitney test; § $p=0.0001$ among all groups in all directions, Kruskal-Wallis test). **(B)** Young's modulus (MPa) of aligned ES collagen scaffolds over time in culture with or without cells (0 day after soaking in $1 \times$ PBS for 1 h, 1 week, and 3 weeks) ($n=6$). (* $p=0.0317$ acellular collagen scaffolds vs. cell-laden collagen scaffolds for 3 weeks, Mann-Whitney test; § $p=0.0074$ among all groups, Kruskal-Wallis test). **(C)** Stress/strain curve for each condition. **(D)** Dotted outlined area of stress/strain curve in (C). **(E)** Ultimate stress readings (MPa) for each condition either crosslinked or noncrosslinked ($n=8$). (* $p=0.0120$ noncrosslinked aligned vs. random collagen scaffolds, ## $p<0.0001$ crosslinked aligned vs. random collagen scaffolds, # $p=0.0240$ crosslinked aligned vs. perpendicular oriented collagen scaffolds, Mann-Whitney test; § $p=0.0001$ among all groups in all directions, Kruskal-Wallis test). **(F)** Ultimate stress (MPa) for aligned ES collagen scaffolds over time in culture with or without cells (0 day after soaking in PBS for 1 h, 1 week, and 3 weeks) ($n=6$) (* $p=0.0159$ acellular collagen scaffolds vs. cell-laden collagen scaffolds for 3 weeks, Mann-Whitney test; § $p=0.0027$ among all groups, Kruskal-Wallis test). NC, noncrosslinked; CL, crosslinked; PBS, phosphate-buffered saline. Color images available online at www.liebertpub.com/tea

spread out with multidirectional extensions (Fig. 1C, E, and G). Cells on aligned collagen scaffolds were elongated in line with the direction of the fibers (Fig. 1D, F, and H). These differences in morphology and alignment were also seen in the confocal images (Fig. 1G, H), which provided evidence of high cell viability in aligned scaffolds.

Mechanical properties of scaffolds influenced by fiber alignment and culture conditions

Crosslinking with GA increased the average tensile modulus of dry random scaffolds from 32.48 ± 11.84 (noncrosslinked) to 57.56 ± 28.11 MPa (Fig. 2A; Table 2). Crosslinking also increased the average tensile modulus of dry aligned collagen fibers when tested in tension parallel, random, or perpendicular to the direction of aligned fibers (Fig. 2A; Table 2). There was significant difference among all dry groups in all directions (Kruskal–Wallis test, $p=0.0001$). However, there was no significant difference between dry-noncrosslinked and dry-crosslinked collagen scaffolds on each direction. Aligned scaffolds, when tested in the direction parallel to the aligned nanofibers generated a significantly greater tensile modulus compared to random scaffolds, regardless of crosslinking (Mann–Whitney test, $p=0.001$ for noncrosslinked collagen scaffolds; $p=0.0005$ for crosslinked collagen scaffolds). On the other hand, the tensile modulus perpendicular to the direction of the aligned fibers was 39.63 ± 19.27 MPa after crosslinking, significantly weaker than aligned scaffolds (Mann–Whitney test, $p=0.0020$). Similar to the tensile modulus, the UTS of crosslinked aligned scaffolds was significantly higher: 4.97 ± 2.01 MPa (parallel to direction of alignment) (Mann–Whitney test, $p=0.0240$) and also compared to 1.19 ± 0.63 MPa measured in the crosslinked random scaffolds (Mann–Whitney test, $p<0.0001$). The stress–strain curves and the ultimate stress values for random and aligned scaffolds (nonfixed or GA fixed) are presented in Figure 2C–E.

Mechanical properties of cell-seeded and acellular scaffolds in culture were significantly lower than dry scaffolds (Kruskal–Wallis test, $p<0.0001$ for Young’s modulus and UTS) (Table 3). The stiffness of both cellular and acellular scaffolds decreased with time in culture. However, cell-seeded scaffolds were consistently stiffer and reached a higher ultimate tensile stress than acellular scaffolds.

TABLE 2. ULTIMATE TENSILE STRENGTH AND YOUNG’S MODULUS (MEGAPASCALS) OF FRESHLY MADE AND NONCULTURED RANDOM AND ALIGNED ELECTROSPUN COLLAGEN SCAFFOLDS

<i>ES nanofiber (type)</i>	<i>Noncross-linked/ crosslinked</i>	<i>Tensile strength (MPa)</i>	<i>Young’s modulus (MPa)</i>
Random collagen	NC	1.16 ± 0.88	32.48 ± 11.84
	CL	1.19 ± 0.63	57.56 ± 28.11
Aligned collagen	NC	4.20 ± 1.81	178.72 ± 78.53
	CL	4.97 ± 2.01	214.76 ± 75.41
Perpendicular to aligned collagen	NC	1.44 ± 0.91	12.15 ± 8.42
	CL	1.51 ± 0.97	39.63 ± 19.27

All mechanical properties expressed as mean \pm standard deviation ($n=8$).

ES, electrospun; NC, noncrosslinked scaffolds; CL, crosslinked scaffolds; MPa, megapascals.

TABLE 3. ULTIMATE TENSILE STRENGTH AND YOUNG’S MODULUS (MEGAPASCALS) OF RANDOM AND ALIGNED ELECTROSPUN COLLAGEN SCAFFOLDS OVER TIME IN CULTURE WITH OR WITHOUT CELLS (1 WEEK AND 3 WEEKS)

<i>Time in culture</i>	<i>Tensile strength (MPa)</i>	<i>Young’s modulus (MPa)</i>
1 week		
No cells and aligned	0.48 ± 0.27	0.78 ± 0.48
Cells and aligned	0.63 ± 0.53	1.51 ± 0.90
3 weeks		
No cells and aligned	0.024 ± 0.029	0.26 ± 0.10
Cells and aligned	0.41 ± 0.67	1.053 ± 0.59

All mechanical properties expressed as mean \pm standard deviation ($n=6$).

Changes in mechanical properties of acellular and cell-seeded collagen scaffolds were measured over time in culture to assess the contribution of newly formed matrix with time in culture (Fig. 2B, F; Table 3). After 1 week, the Young’s modulus of the cell-seeded collagen scaffolds was 1.51 ± 0.90 MPa, in comparison to acellular scaffolds (0.78 ± 0.48 MPa). After 3 weeks, the cell-seeded collagen scaffolds generated a significantly greater Young’s modulus of 1.053 ± 0.59 MPa, compared to acellular scaffolds with the Young’s modulus of 0.26 ± 0.098 MPa ($p=0.0317$, Mann–Whitney test). The Young’s modulus and UTS were significantly different in acellular scaffolds and cell-laden scaffolds for 0 day, 1 week, and 3 weeks (Kruskal–Wallis test, $p=0.0074$ for Young’s modulus; $p=0.0027$ for UTS).

To determine whether the increased mechanical property of cell-seeded scaffolds was due to the deposition of newly formed collagen, we used ELISA to measure newly synthesized collagen type I (Fig. 3A). No collagen was detected in the acellular scaffolds since the antibody does not recognize denatured collagen in the scaffold (according to manufacturer’s specification), which was confirmed by our immunostains (Fig. 4M, N). In addition, cells seeded on collagen I scaffolds generated greater levels of collagen I than cells seeded on PLA (Fig. 3A).

A meniscal-like phenotype is supported by ES scaffolds and specific gene responses differed between cell source and scaffold organization

In comparison to meniscal cells in monolayer culture (baseline gene expression levels indicated by dotted line in Fig. 3B–F), cells that were derived from either vascular or avascular regions cultivated on both random and aligned collagen scaffolds expressed significantly higher levels of *COL1A1*, *SOX9*, *COMP*, *CHAD*, and *AGG* gene expression relative to monolayer cultured cells (Kruskal–Wallis test, $p<0.05$). Although *COL1A1* and *AGG* mRNA expression levels were higher for both meniscus cell sources on aligned scaffolds relative to random oriented scaffolds (Kruskal–Wallis test, $p=0.0026$ for *COL1A1*; $p=0.0441$ for *AGG*) (Fig. 3B, F), no significant differences in gene expression levels were found between vascular and avascular cells.

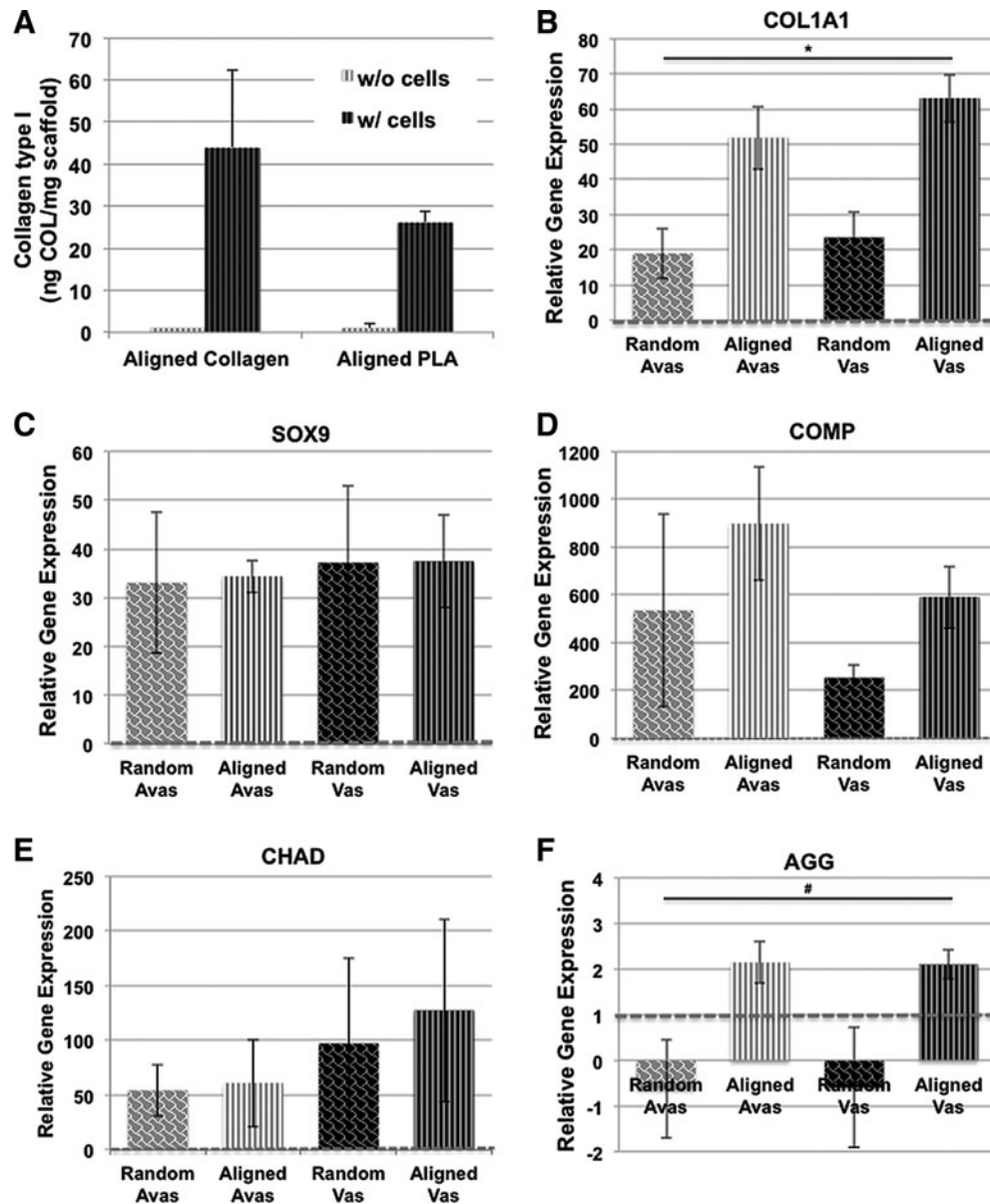


FIG. 3. ELISA quantification for collagen type I and gene expression levels of human vascular and avascular meniscus cells cultivated on either random or aligned collagen ES scaffolds. (A) ELISA quantification of collagen type I for cell- and noncell-seeded aligned collagen and PLA scaffolds. (B) *COL1A1* gene expression. (* $p=0.0026$ among experimental groups, Kruskal–Wallis test). (C) *SOX9* gene expression. (D) *COMP* gene expression. (E) *CHAD* gene expression. (F) *Aggrecan* gene expression (# $p=0.0441$ among experimental groups, Kruskal–Wallis test) ($n=4–6$ donors) relative to monolayer controls. Expression levels are relative to monolayer controls (red dotted line). Cells that were derived from either vascular or avascular regions cultivated on both random and aligned collagen scaffolds expressed significantly ($p<0.05$, Kruskal–Wallis test) higher levels of *COL1A1*, *SOX9*, *COMP*, *CHAD*, and *AGG* gene expression relative to monolayer cultured cells. ELISA, enzyme-linked immunosorbent assay.

Integration and neotissue formation of ES cell-seeded scaffolds in an ex vivo meniscus defect model

Human meniscal cells seeded on collagen-aligned scaffolds and precultured for 4 weeks were implanted in surgically created longitudinal tears in bovine meniscus tissue explants. After 3 weeks of post-repair culture in six-well plates, histological analysis revealed the generation of newly formed tissue within the tear. The repair tissue consisted of cells with elongated cellular morphology, collagen

type I positive matrix staining (IHC), and evidence of scaffold/neotissue integration within the defect (Fig. 4). Histomorphometry on collagen ES scaffolds seeded with human meniscus avascular cells showed 90% integration with host meniscus tissue and was markedly greater than acellular collagen scaffolds (Fig. 4O–Q). MRI of the *ex vivo* repair (Fig. 5A–F) revealed persistence of the surgical tear in the unrepaired group. Apposition without integration of the interface in the acellular scaffold group was observed. Integration of the scaffold into host tissue in the cell-seeded

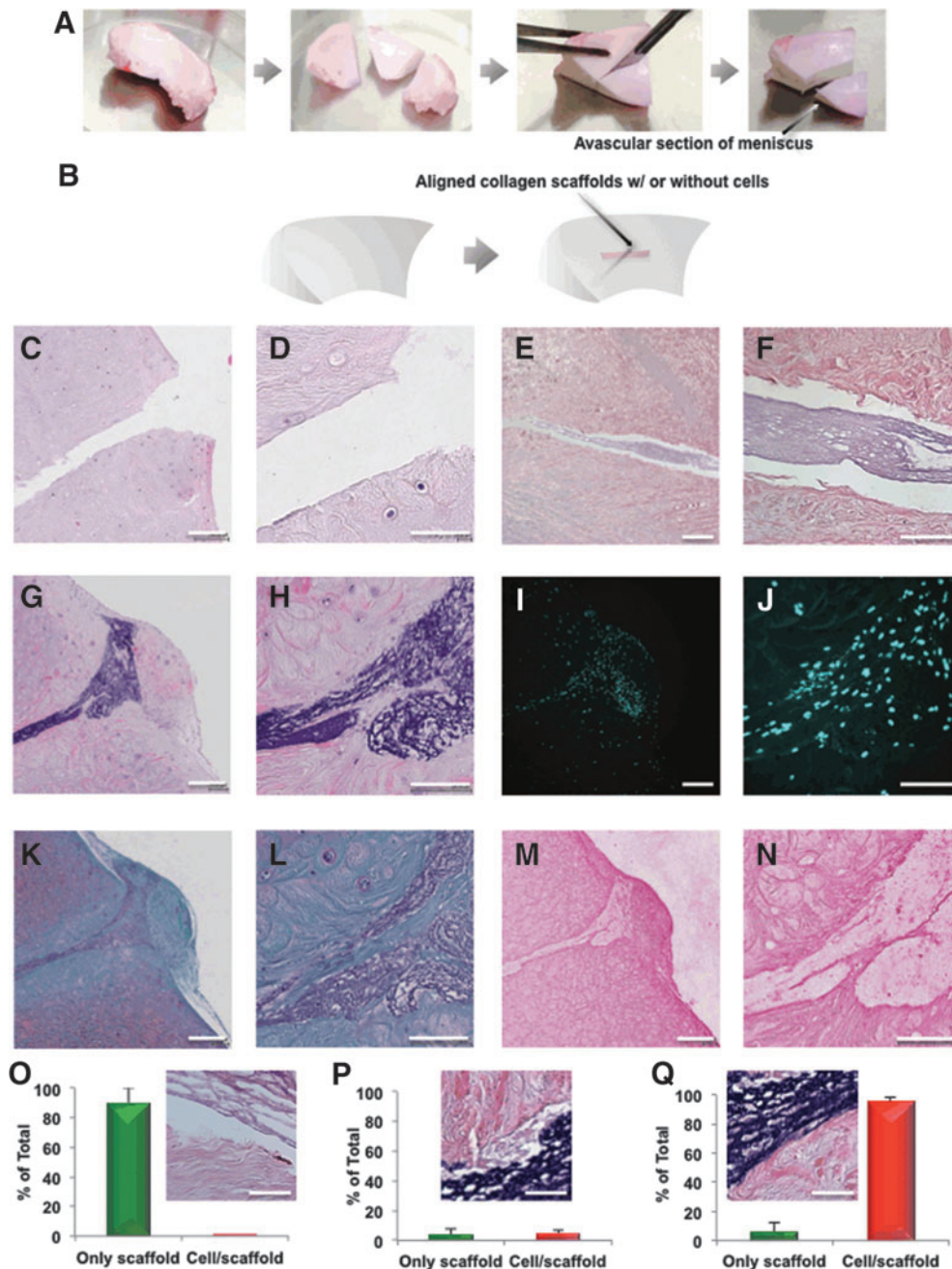


FIG. 4. Overview of the bovine meniscus *ex vivo* repair model: creation, histology, and histomorphometric analysis. **(A)** Fabrication of avascular section of meniscus. **(B)** Coronal defects were surgically produced in bovine meniscus white zone tissue and 4-week-old meniscus avascular cell-seeded aligned collagen scaffolds were inserted and cultured for a further 3 weeks. Nontreated defects and non-cell seeded collagen scaffolds were used as controls. The scaffold was placed within the coronal defect of bovine meniscal avascular zone. All constructs were cultured for 3 weeks and then processed for histology. **(C, D)** H&E stain of only defect in meniscus. **(E, F)** H&E stain of only collagen implant. **(G, H)** H&E stain of the cells/aligned collagen scaffold implant within the defect of meniscus. **(I, J)** DAPI stain of the cells/aligned collagen scaffold implant. **(K, L)** Safranin O/fast-green stain of the cells/aligned collagen scaffold implant. **(M, N)** Collagen type I immunostaining of the cells/aligned collagen scaffold implant. [Mag. **(C, E, G, I, K)**, and **(M)**=10 \times , scale bar: 200 μ m; Mag. **(D, F, H, J, L)**, and **(N)**=40 \times , scale bar: 100 μ m]. Histomorphometric analysis of meniscus integration in the above histological sections: **(O)** the % disintegration ($p < 0.0001$), **(P)** the % apposition (no significant difference), and **(Q)** the % integration ($p < 0.0001$) (scale bar: 50 μ m). The % of disintegration, apposition, or integration divided into each morphological group was calculated according to Pabbruwe's study.^{38,39} DAPI, 4',6-diamidino-2-phenylindole; H&E, hematoxylin and eosin. Color images available online at www.liebertpub.com/tea

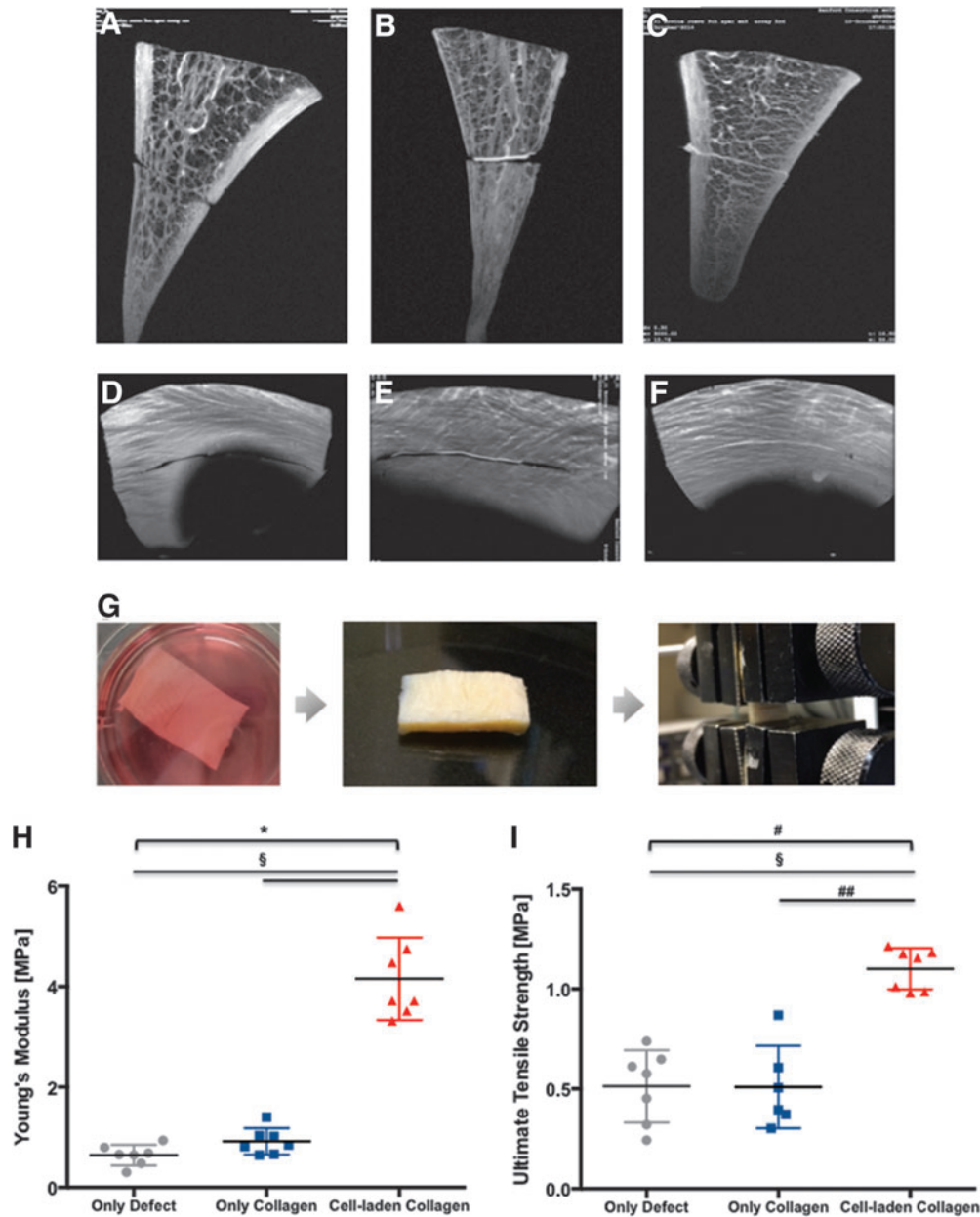


FIG. 5. MRI images and mechanical strength of bovine meniscus *ex vivo* repair model. Collagen membranes were seeded with human meniscus avascular cells to create human meniscus avascular cells/ES collagen scaffold implant, as described under section “Materials and Methods”. The scaffolds were inserted into incisions made in a bovine meniscus avascular section and cultured for 3 weeks. MRI images of meniscal specimens in coronal plane to the meniscus with (A) defect without any repair, (B) defect repaired with acellular aligned ES scaffold, and (C) defect repaired with cell-seeded aligned ES scaffold. Imaging of meniscus specimens in the axial plane to the meniscus with (D) defect without any repair, (E) defect repaired with acellular aligned ES scaffold, and (F) defect repaired with cell-seeded aligned ES scaffold. Mechanical strength of integrated meniscus: (G) Images of the cell-seeded collagen scaffold implant during culturing, harvesting, and the tensile testing process; (H) Young’s modulus ($n=7$) ($*p<0.0001$ among experimental groups, Kruskal–Wallis test; $§p=0.0006$ defects without any repair and repaired with acellular aligned ES scaffold vs. defects repaired with cell-seeded aligned ES scaffold, Mann–Whitney test) and (I) ultimate tensile strength of meniscal repair model comparing defects repaired with cell-seeded aligned ES scaffold to defects without any repair and defects repaired with acellular aligned ES scaffold ($n=7$) ($^{\#}p=0.0001$ among experimental groups, Kruskal–Wallis test; $§p=0.0006$ defects without any repair vs. defects repaired with cell-seeded aligned ES scaffold, Mann–Whitney test; $^{\#\#}p=0.0012$ defects repaired with acellular aligned ES scaffold vs. defects repaired with cell-seeded aligned ES scaffold, Mann–Whitney test). MRI, magnetic resonance imaging. Color images available online at www.liebertpub.com/tea

scaffold group can be detected. On mechanical testing of the repaired defects, cell-seeded scaffolds possessed significantly greater tensile mechanical properties (Young's modulus = 4.16 ± 0.82 MPa and UTS = 1.10 ± 0.10 MPa) compared to either unrepaired defects (Young's modulus = 0.64 ± 0.20 MPa and UTS = 0.51 ± 0.18 MPa, Mann-Whitney test, $p = 0.0006$) or defects repaired with acellular scaffolds (Young's modulus = 0.92 ± 0.26 MPa, Mann-Whitney test, $p = 0.0012$, and UTS = 0.51 ± 0.20 MPa, Mann-Whitney test, $p = 0.0006$) in Figure 5G–I. The differences across all three groups were significant (Kruskal-Wallis test; $p = 0.0001$ for UTS; $p < 0.0001$ for Young's modulus).

Discussion

A meniscal tear is the most frequently recorded diagnosis of all orthopedic diagnoses, and partial or total meniscectomy remains the most common of all orthopedic procedures.⁴⁰ Electrospinning is an attractive tissue fabrication process to generate nanofibrous scaffolds that emulate the structure of native meniscal tissue. We have shown that collagen ES scaffolds produced in this study support the viability of human meniscus cells, induced an organized cellular alignment reflecting the scaffold microstructure, and promoted the formation of meniscus-like tissues. Prefabrication of organized collagen scaffolds with an architecture mimicking the meniscus collagen bundle organization showed promise for the repair of meniscal tears, as demonstrated by the formation and integration of new tissue in the *ex vivo* meniscus defect model.

Fabrication of scaffolds for meniscus tissue engineering by electrospinning has been accomplished with numerous synthetic as well as natural biopolymers.⁴¹ We have also previously shown proof of concept of engineering meniscogenic tissue by electrospinning PLA.²⁸ Despite the biocompatibility and mechanical properties of ES PLA, there is some concern about the reduction in pH induced by biodegradation products (lactic acid) within the knee joint as noted by others using this material.³⁰ In this study, we selected collagen type I to more closely mimic the dominant structural protein in native meniscal tissue. Using collagen type I scaffolds also appeared to be advantageous for tissue engineering since it leads to a higher production of collagen type I compared to PLA scaffolds. Similar to our previous report on PLA scaffolds,²⁸ we also observed that the aligned ES collagen scaffolds possessed greater mechanical properties relative to the random ES scaffolds and also generated a higher quality of neotissue (based on gene expression).

The neotissue produced on the collagen scaffolds appeared meniscus-like with a characteristic deposition of collagen type I, high expression of *SOX9*, *COMP*, and *CHAD*, and low GAG content as reported elsewhere for native^{42–44} and engineered meniscus.^{28,45–47} Although scaffolds were composed of collagen type I, we confirmed that the antibody for immunostaining and ELISA was specific to newly synthesized collagen type I by comparing results to acellular scaffolds. In addition, meniscal cells seeded on collagen I ES scaffolds generated greater levels of collagen I than cells seeded on PLA, supporting our rationale for selecting a naturally occurring polymer.

Electrospinning is a convenient manufacturing technique for tuning the anisotropy of tissue engineering scaffolds and

mechanical properties. Dry extruded collagen fibers have a wide range of reported tensile moduli: from 2 to 46 MPa⁴⁸ to 1.7 to 3.3 GPa.⁴⁹ Dry ES collagen scaffolds had a reported tensile modulus of 52 MPa in the dominant direction of fiber alignment and 26 MPa in the direction perpendicular to fiber alignment.⁵⁰ The moduli of our dry ES mats, even before crosslinking, were substantially greater. Single ES collagen fibers have a reported bending modulus of 1.3–7.8 GPa. However, the bending modulus decreased dramatically after hydration in the PBS buffer (to 0.07–0.26 MPa).⁵¹ Crosslinking with GA almost doubled the shear modulus of single ES collagen fibers and rendered the fibers insoluble.⁵¹ GA has also been shown to effectively increase the tensile strength of extruded collagen threads.⁵² In our study, crosslinking with GA doubled the stiffness of randomly aligned collagen and increased the stiffness of aligned collagen by 120%.

Upon hydration, noncrosslinked scaffolds quickly lost most of their structural integrity, while GA-crosslinked scaffolds remained intact. However, upon culture, the mechanical properties of hydrated scaffolds were significantly reduced. Interestingly, the mechanical properties of the cell-seeded scaffolds at weeks 1 and 3 did not significantly change over time. The 3-week-cultured cell-seeded scaffolds possessed a significantly greater Young's modulus (0.90 ± 0.62 MPa) compared to the acellular scaffolds at the same time point (0.26 ± 0.10 MPa). The difference in mechanical properties between cell-seeded and acellular scaffolds was most likely due to collagen type I deposition as documented by IHC and ELISA. Furthermore, these cell-seeded collagen scaffolds had a much higher tensile mechanical property than previously reported for protein polymer scaffold. For example, Grogan *et al.*⁴⁷ reported that methacrylated gelatin scaffolds patterned by projection stereolithography possessed a Young's modulus of about 0.01 MPa. On noncell-seeded scaffolds, Kai *et al.*⁵³ measured tensile properties of a blend of coaxial PCL/gelatin ES nanofibers. After soaking in PBS for 3 h, the Young's modulus was only 0.13 ± 0.04 MPa and 0.56 ± 0.09 MPa. Grover *et al.*⁵⁴ varied the ratio of collagen to gelatin in their scaffolds to tailor their mechanical and degradation properties. Pure collagen, pure gelatin, and mixed collagen-gelatin 1:1 scaffolds had a Young's modulus of 81 ± 8 kPa, 4.6 ± 0.1 kPa, and 19 ± 3 kPa, respectively. The Young's modulus of pure collagen scaffolds was the highest measured among seven different scaffolds tested on that study. The tensile moduli of our cell-seeded collagen scaffolds were consistently higher than that previously reported for scaffolds of collagen origin.

Puetzer *et al.*⁵⁵ encapsulated meniscus cells in a hydrogel and subjected them under strain using a mechanical anchoring system. They reported increased mechanical properties of up to 160 kPa over 8 weeks in culture. Although, we did not observe an increase in mechanical properties of our cell-seeded scaffolds between 1 and 3 weeks, the range of Young's modulus generated by our scaffolds was 1–1.5 MPa, almost 10 times greater than that reported by Puetzer *et al.*⁵⁵ The noncell-seeded scaffolds degraded and lost mechanical strength, as previously reported for other collagen-based scaffolds^{56,57} and other biodegradable scaffold systems such as poly (ethylene oxide) (PEO), poly(lactic-co-glycolic acid) (PLGA), and

mixes of PCL/PLGA.⁵⁸ Modification of collagen scaffolds, such as combining with glycosaminoglycans, can retard degradation rates⁵⁶ and may be an approach to use with our collagen scaffold for meniscus repair.

Cell-seeded scaffolds can generate additional extracellular matrix after implantation and therefore tend to integrate better into host tissue.⁵⁹ Kobayashi *et al.* reported that meniscal grafts from the vascular region had a better repair capacity than grafts from the avascular region, suggesting an intrinsic repair capacity independent of blood supply.⁶⁰ On the other hand, Hennerbichler *et al.* did not find any significant difference in the repair capacity between vascular and avascular zones.⁶¹ In our experiments, we also did not find significant differences in gene expression between meniscal cells harvested from vascular and avascular regions. We therefore chose to only study avascular cells in the *ex vivo* repair model.

The *ex vivo* tear repair model developed in this study supports the potential for cell-seeded collagen scaffolds to integrate with native tissues. After 2 weeks, we were able to form integrated repair tissue with a Young's modulus of 4.16 ± 0.82 MPa. Others have also reported on *ex vivo* repair of meniscal tears. Pabbruwe *et al.* seeded commercial sources of collagen membranes or sponges with bone marrow-derived mesenchymal stem cell and after 40 days created repair tissues with a tensile strength of 30 MPa.³⁸ Qu *et al.*⁶² developed collagenase-releasing scaffolds implant with bovine meniscus and after 50 days showed an integration strength of PCL/PEO with low-dose collagenase of <15 kPa. More recently, Shimomura *et al.*, reported on the repair of radial meniscal tears using ES PCL scaffolds made porous by sacrificial PEO and seeded with bovine meniscal fibrochondrocytes.⁶³ In that study, however, the meniscal explants were wrapped by the scaffolds at the site of the tear and created repair tissue with a Young's modulus of 12.5 MPa over 8 weeks in culture. Overall, a direct comparison of the mechanical properties derived from these repair model studies is difficult because of the differences in the creation of tears or meniscal defects, the repair procedure, and the methods of testing. However, our data show a significantly increased mechanical property after only 2 weeks.

Despite the positive interaction of human meniscus cells with the collagen scaffolds, the low toxicity, and encouraging new tissue formation, several issues remain to be addressed before potential application for enhancement of meniscal tissue repair. We are continuing to enhance the biomechanical function by optimizing electrospinning and crosslinking conditions, by enhancing cell culture, and by combining collagen with other biomaterials. While fibrochondrocytes have been extensively tested with some success, we are also exploring other cell sources, such as bone marrow-derived mesenchymal stem cells, that are more attractive because the source of meniscal fibrochondrocytes is limited.³⁸

In summary, we used ES collagen scaffolds to induce a cellular alignment with scaffold microstructure and stimulate meniscogenic neotissue formation. Collagen scaffolds mimicking the collagen bundle organization of the native meniscus have promise for the repair of meniscal tears, as indicated by the generation and integration of new tissue in *ex vivo* meniscal tears in the avascular region.

Acknowledgments

Funding was provided by the National Institutes of Health (P01 AG007996), the Shaffer Family Foundation, and Donald and Darlene Shiley. We are grateful to the efforts by Judy Blake (copyediting), Dr. Wonchul Choi (technical support for the *ex vivo* model), and Drs. Graeme Bydder and Hongda Shao (MRI analyses).

Author Contributions

J.B., S.J., S.P.G., and D.D.D. designed the study and wrote the article in close collaboration with the other authors. J.B. and S.S. conducted cell culture studies and conducted histology and qPCR analyses. J.B. conducted and interpreted the SEM analysis. J.B. and N.E.G. conducted the *ex vivo* repair model. J.D. provided the MRI imaging. All authors discussed the results and approved the final version of the article.

Disclosure Statement

No competing financial interests exist.

References

1. Sweigart, M.A., and Athanasiou, K.A. Toward tissue engineering of the knee meniscus. *Tissue Eng* **7**, 111, 2001.
2. Boyd, K.T., and Myers, P.T. Meniscus preservation; rationale, repair techniques and results. *Knee* **10**, 1, 2003.
3. Baker, P., Coggon, D., Reading, I., Barrett, D., McLaren, M., and Cooper, C. Sports injury, occupational physical activity, joint laxity, and meniscal damage. *J Rheumatol* **29**, 557, 2002.
4. Majewski, M., Susanne, H., and Klaus, S. Epidemiology of athletic knee injuries: a 10-year study. *Knee* **13**, 184, 2006.
5. van Tienen, T.G., Hannink, G., and Buma, P. Meniscus replacement using synthetic materials. *Clin Sports Med* **28**, 143, 2009.
6. Lozano, J., Ma, C.B., and Cannon, W.D. All-inside meniscus repair: a systematic review. *Clin Orthop Relat Res* **455**, 134, 2007.
7. Roos, H., Lauren, M., Adalberth, T., Roos, E.M., Jonsson, K., and Lohmander, L.S. Knee osteoarthritis after meniscectomy: prevalence of radiographic changes after twenty-one years, compared with matched controls. *Arthritis Rheum* **41**, 687, 1998.
8. Englund, M., Guermazi, A., Roemer, F.W., Yang, M., Zhang, Y., Nevitt, M.C., *et al.* Meniscal pathology on MRI increases the risk for both incident and enlarging subchondral bone marrow lesions of the knee: the MOST Study. *Ann Rheum Dis* **69**, 1796, 2010.
9. Ibarra, C., Koski, J.A., and Warren, R.F. Tissue engineering meniscus: cells and matrix. *Orthop Clin North Am* **31**, 411, 2000.
10. McCarty, E.C., Marx, R.G., and DeHaven, K.E. Meniscus repair: considerations in treatment and update of clinical results. *Clin Orthop Relat Res* **402**, 122, 2002.
11. Port, J., Jackson, D.W., Lee, T.Q., and Simon, T.M. Meniscal repair supplemented with exogenous fibrin clot and autogenous cultured marrow cells in the goat model. *Am J Sports Med* **24**, 547, 1996.
12. Peretti, G.M., Gill, T.J., Xu, J.W., Randolph, M.A., Morse, K.R., and Zaleske, D.J. Cell-based therapy for meniscal repair: a large animal study. *Am J Sports Med* **32**, 146, 2004.

13. Izuta, Y., Ochi, M., Adachi, N., Deie, M., Yamasaki, T., and Shinomiya, R. Meniscal repair using bone marrow-derived mesenchymal stem cells: experimental study using green fluorescent protein transgenic rats. *Knee* **12**, 217, 2005.
14. Walsh, C.J., Goodman, D., Caplan, A.I., and Goldberg, V.M. Meniscus regeneration in a rabbit partial meniscectomy model. *Tissue Eng* **5**, 327, 1999.
15. Cook, J.L., Fox, D.B., Malaviya, P., Tomlinson, J.L., Kuroki, K., Cook, C.R., *et al.* Long-term outcome for large meniscal defects treated with small intestinal submucosa in a dog model. *Am J Sports Med* **34**, 32, 2006.
16. Stapleton, T.W., Ingram, J., Fisher, J., and Ingham, E. Investigation of the regenerative capacity of an acellular porcine medial meniscus for tissue engineering applications. *Tissue Eng Part A* **17**, 231, 2011.
17. Bruns, J., Kahrs, J., Kampen, J., Behrens, P., and Plitz, W. Autologous perichondral tissue for meniscal replacement. *J Bone Joint Surg Br* **80**, 918, 1998.
18. Bodin, A., Concaro, S., Brittberg, M., and Gatenholm, P. Bacterial cellulose as a potential meniscus implant. *J Tissue Eng Regen Med* **1**, 406, 2007.
19. Calve, S., Dennis, R.G., Kosnik, P.E., 2nd, Baar, K., Grosh, K., and Arruda, E.M. Engineering of functional tendon. *Tissue Eng* **10**, 755, 2004.
20. Zhang, Y.Z., Su, B., Venugopal, J., Ramakrishna, S., and Lim, C.T. Biomimetic and bioactive nanofibrous scaffolds from electrospun composite nanofibers. *Int J Nanomedicine* **2**, 623, 2007.
21. Kumbhar, S.G., Nukavarapu, S.P., James, R., Nair, L.S., and Laurencin, C.T. Electrospun poly(lactic acid-co-glycolic acid) scaffolds for skin tissue engineering. *Biomaterials* **29**, 4100, 2008.
22. McClure, M.J., Sell, S.A., Simpson, D.G., and Bowlin, G.L. Electrospun polydioxanone, elastin, and collagen vascular scaffolds: uniaxial cyclic distension. *J Eng Fiber Fabr* **4**, 18, 2009.
23. Li, M., Mondrinos, M.J., Gandhi, M.R., Ko, F.K., Weiss, A.S., and Lelkes, P.I. Electrospun protein fibers as matrices for tissue engineering. *Biomaterials* **26**, 5999, 2005.
24. Homayoni, H., Ravandi, S.A.H., and Valizadeh, M. Electrospinning of chitosan nanofibers: processing optimization. *Carbohydr Polym* **77**, 656, 2009.
25. Kumbhar, S.G., Nukavarapu, S.P., James, R., Hogan, M.V., and Laurencin, C.T. Recent patents on electrospun biomedical nanostructures: an overview. *Recent Pat Biomed Eng* **1**, 68, 2008.
26. Platt, M.A. Tendon repair and healing. *Clin Podiatr Med Surg* **22**, 553, 2005.
27. Dong, B., Arnoult, O., Smith, M.E., and Wnek, G.E. Electrospinning of collagen nanofiber scaffolds from benign solvents. *Macromol Rapid Commun* **30**, 539, 2009.
28. Baek, J., Chen, X., Sovani, S., Jin, S., Grogan, S.P., and D'Lima, D.D. Meniscus tissue engineering using a novel combination of electrospun scaffolds and human meniscus cells embedded within an extracellular matrix hydrogel. *J Orthop Res* **33**, 572, 2015.
29. Bergsma, E.J., Rozema, F.R., Bos, R.R.M., and De Bruijn, W.C. Foreign body reactions to resorbable poly(l-lactide) bone plates and screws used for the fixation of unstable zygomatic fractures. *J Oral Maxillofac* **51**, 666, 1993.
30. Spain, T.L., Agrawal, C.M., and Athanasiou, K.A. New technique to extend the useful life of a biodegradable cartilage implant. *Tissue Eng* **4**, 343, 1998.
31. Makris, E.A., Hadidi, P., and Athanasiou, K.A. The knee meniscus: structure-function, pathophysiology, current repair techniques, and prospects for regeneration. *Biomaterials* **32**, 7411, 2011.
32. Huang, L., Nagapudi, K., Apkarian, R.P., and Chaikof, E.L. Engineered collagen-PEO nanofibers and fabrics. *J Biomater Sci Polym Ed* **12**, 979, 2001.
33. Roberts, S., Menage, J., Sandell, L.J., Evans, E.H., and Richardson, J.B. Immunohistochemical study of collagen types I and II and procollagen IIA in human cartilage repair tissue following autologous chondrocyte implantation. *Knee* **16**, 398, 2009.
34. Pauli, C., Grogan, S.P., Patil, S., Otsuki, S., Hasegawa, A., Koziol, J., *et al.* Macroscopic and histopathologic analysis of human knee menisci in aging and osteoarthritis. *Osteoarthritis Cartilage* **19**, 1132, 2011.
35. Barbero, A., Grogan, S., Schafer, D., Heberer, M., Mainil-Varlet, P., and Martin, I. Age related changes in human articular chondrocyte yield, proliferation and post-expansion chondrogenic capacity. *Osteoarthritis Cartilage* **12**, 476, 2004.
36. Martin, I., Jakob, M., Schafer, D., Dick, W., Spagnoli, G., and Heberer, M. Quantitative analysis of gene expression in human articular cartilage from normal and osteoarthritic joints. *Osteoarthritis Cartilage* **9**, 112, 2001.
37. Grogan, S.P., Miyaki, S., Asahara, H., D'Lima, D.D., and Lotz, M.K. Mesenchymal progenitor cell markers in human articular cartilage: normal distribution and changes in osteoarthritis. *Arthritis Res Ther* **11**, R85, 2009.
38. Pabbruwe, M.B., Kafienah, W., Tarlton, J.F., Mistry, S., Fox, D.J., and Hollander, A.P. Repair of meniscal cartilage white zone tears using a stem cell/collagen-scaffold implant. *Biomaterials* **31**, 2583, 2010.
39. Pabbruwe, M.B., Esfandiari, E., Kafienah, W., Tarlton, J.F., and Hollander, A.P. Induction of cartilage integration by a chondrocyte/collagen-scaffold implant. *Biomaterials* **30**, 4277, 2009.
40. Garrett, W.E., Jr., Swiontkowski, M.F., Weinstein, J.N., Callaghan, J., Rosier, R.N., Berry, D.J., *et al.* American Board of Orthopaedic Surgery Practice of the Orthopaedic Surgeon: part-II, certification examination case mix. *J Bone Joint Surg Am* **88**, 660, 2006.
41. Rim, N.G., Shin, C.S., and Shin, H. Current approaches to electrospun nanofibers for tissue engineering. *Biomed Mater* **8**, 014102, 2013.
42. Cheung, H.S. Distribution of type I, II, III and V in the pepsin solubilized collagens in bovine menisci. *Connect Tissue Res* **16**, 343, 1987.
43. Eyre, D.R., and Wu, J.J. Collagen of fibrocartilage: a distinctive molecular phenotype in bovine meniscus. *FEBS Lett* **158**, 265, 1983.
44. Kambic, H.E., and McDevitt, C.A. Spatial organization of types I and II collagen in the canine meniscus. *J Orthop Res* **23**, 142, 2005.
45. Freymann, U., Endres, M., Neumann, K., Scholman, H.J., Morawietz, L., and Kaps, C. Expanded human meniscus-derived cells in 3-D polymer-hyaluronan scaffolds for meniscus repair. *Acta Biomater* **8**, 677, 2012.
46. Xu, T., Binder, K.W., Albanna, M.Z., Dice, D., Zhao, W., Yoo, J.J., *et al.* Hybrid printing of mechanically and biologically improved constructs for cartilage tissue engineering applications. *Biofabrication* **5**, 015001, 2013.
47. Grogan, S.P., Chung, P.H., Soman, P., Chen, P., Lotz, M.K., Chen, S., *et al.* Digital micromirror device projection

- printing system for meniscus tissue engineering. *Acta Biomater* **9**, 7218, 2013.
48. Pins, G.D., Christiansen, D.L., Patel, R., and Silver, F.H. Self-assembly of collagen fibers. Influence of fibrillar alignment and decorin on mechanical properties. *Biophys J* **73**, 2164, 1997.
 49. Zeugolis, D.I., Paul, G.R., and Attenburrow, G. Cross-linking of extruded collagen fibers—a biomimetic three-dimensional scaffold for tissue engineering applications. *J Biomed Mater Res A* **89**, 895, 2009.
 50. Matthews, J.A., Wnek, G.E., Simpson, D.G., and Bowlin, G.L. Electrospinning of collagen nanofibers. *Biomacromolecules* **3**, 232, 2002.
 51. Yang, L., Fitie, C.F., van der Werf, K.O., Bennink, M.L., Dijkstra, P.J., and Feijen, J. Mechanical properties of single electrospun collagen type I fibers. *Biomaterials* **29**, 955, 2008.
 52. Cavallaro, J.F., Kemp, P.D., and Kraus, K.H. Collagen fabrics as biomaterials. *Biotechnol Bioeng* **43**, 781, 1994.
 53. Kai, D., Prabhakaran, M.P., Stahl, B., Eblenkamp, M., Wintermantel, E., and Ramakrishna, S. Mechanical properties and in vitro behavior of nanofiber-hydrogel composites for tissue engineering applications. *Nanotechnology* **23**, 095705, 2012.
 54. Grover, C.N., Cameron, R.E., and Best, S.M. Investigating the morphological, mechanical and degradation properties of scaffolds comprising collagen, gelatin and elastin for use in soft tissue engineering. *J Mech Behav Biomed Mater* **10**, 62, 2012.
 55. Puetzer, J.L., Koo, E., and Bonassar, L.J. Induction of fiber alignment and mechanical anisotropy in tissue engineered menisci with mechanical anchoring. *J Biomech* **48**, 1436.
 56. Yannas, I.V., Tzeranis, D.S., Harley, B.A., and So, P.T.C. Biologically active collagen-based scaffolds: advances in processing and characterization. *Philos Trans A Math Phys Eng Sci* **368**, 2123, 2010.
 57. Barnes, C.P., Pemble IV, C.W., Brand, D.D., Simpson, D.G., and Bowlin, G.L. Cross-linking electrospun type II collagen tissue engineering scaffolds with carbodiimide in ethanol. *Tissue Eng* **13**, 1593, 2007.
 58. Baker, B.M., Nerurkar, N.L., Burdick, J.A., Elliott, D.M., and Mauck, R.L. Fabrication and modeling of dynamic multipolymer nanofibrous scaffolds. *J Biomech Eng* **131**, 101012, 2009.
 59. Angele, P., Johnstone, B., Kujat, R., Zellner, J., Nerlich, M., Goldberg, V., *et al.* Stem cell based tissue engineering for meniscus repair. *J Biomed Mater Res A* **85**, 445, 2008.
 60. Kobayashi, K., Fujimoto, E., Deie, M., Sumen, Y., Ikuta, Y., and Ochi, M. Regional differences in the healing potential of the meniscus—an organ culture model to eliminate the influence of microvasculature and the synovium. *Knee* **11**, 271, 2004.
 61. Hennerbichler, A., Moutos, F.T., Hennerbichler, D., Weinberg, J.B., and Guilak, F. Repair response of the inner and outer regions of the porcine meniscus in vitro. *Am J Sports Med* **35**, 754, 2007.
 62. Qu, F., Lin, J.-M.G., Esterhai, J.L., Fisher, M.B., and Mauck, R.L. Biomaterial-mediated delivery of degradative enzymes to improve meniscus integration and repair. *Acta Biomater* **9**, 6393, 2013.
 63. Shimomura, K., Bean, A.C., Lin, H., Nakamura, N., and Tuan, R.S. In vitro repair of meniscal radial tear using aligned electrospun nanofibrous scaffold. *Tissue Eng Part A* **21**, 2066, 2015.

Address correspondence to:

Darryl D. D'Lima, MD, PhD

Shiley Center for Orthopaedic Research
and Education at Scripps Clinic
11025 North Torrey Pines Road, Suite 200
La Jolla, CA 92037

E-mail: ddlima@scripps.edu

Received: June 18, 2015

Accepted: January 19, 2016

Online Publication Date: March 2, 2016